Regression of Lung Cancer by Hypoxia Sensitizing Ruthenium Polypyridyl Complexes

Abhishek Yadav[1], Thamara Janaratne[1], Arthi Krishnan[1], Sharad S. Singhal[2], Sushma Yadav[2],

Adam S. Dayoub[1], Doyle L. Hawkins,[3] Sanjay Awasthi[2*], and Frederick M. MacDonnell[1,*]

[1]Department of Chemistry and Biochemistry, University of Texas at Arlington, Arlington, Texas

[2]Beckman Research Institute, City of Hope Comprehensive Cancer Center, Duarte, California

[3]Department of Mathematics, University of Texas at Arlington, Arlington, Texas

Journal Category: Research Article

Keywords: Ruthenium, lung cancer, hypoxia, tumor xenografts.

Running Title: Hypoxia Sensitizing Ruthenium Polypyridyl Complexes

*Address correspondence to: Frederick M. MacDonnell, Professor, Department of

Chemistry and Biochemistry, 302 Chemistry Research Building, University of Texas at Arlington,

Arlington, TX 76019, Phone: 817-272-2972; Fax: 817-272-3808; Email: macdonn@uta.edu; or

Sanjay Awasthi, Professor, Beckman Research Institute, City of Hope Comprehensive Cancer

Center, Duarte, CA 91010, Phone: 626-256-4673 ext. 31118; Fax: 626-301-8136; Email:

sawasthi@coh.org

Conflicts of Interest: None

ABSTRACT

The ruthenium (II) polypyridyl complexes (RPCs) Δ-[(phen)$_2$Ru(tatpp)]Cl$_2$ (Δ-[**3**]Cl$_2$) and $\Delta\Delta$-[(phen)$_2$Ru(tatpp)Ru(phen)$_2$]Cl$_4$ ($\Delta\Delta$-[**4**]Cl$_4$) are a new generation of metal-based anti-tumor agents. These RPCs bind DNA via intercalation of the tatpp ligand which itself is redox-active and easily reduced at biologically relevant potentials. We have previously shown that RPC **4**$^{4+}$ cleaves DNA when reduced by glutathione to a radical species, and that this DNA cleavage is potentiated under hypoxic conditions in vitro. Here we show that **3**$^{2+}$ also exhibits free-radical mediated DNA cleavage in vitro, and that **3**$^{2+}$ and **4**$^{4+}$ both exhibit selective cytotoxicity towards cultured malignant cell lines, and marked inhibition of tumor growth in vivo. The murine acute toxicity of RPCs **3**$^{2+}$ and **4**$^{4+}$ (maximum tolerable doses (MTD's) ~ 65 μmol/kg) is comparable with that for cisplatin (LD$_{50}$ ~57 μmol/kg) but unlike cisplatin, RPC's are generally cleared from the body unchanged via renal excretion without appreciable metabolism or nephrotoxic side effects. RPCs **3**$^{2+}$ and **4**$^{4+}$ are demonstrated to suppress growth of human non-small cell lung carcinoma (~83%), show potentiated cytotoxicity in vitro under hypoxic conditions, and induce apoptosis through both intrinsic and extrinsic pathways. The novel hypoxia-enhanced DNA cleavage activity and biological activity suggest a promising new anti-cancer pharmacophore based on metal complexes with aromatic ligands that are easily reduced at biologically accessible potentials.

INTRODUCTION

The success of cisplatin (cis-Pt(NH$_3$)$_2$Cl$_2$) as a chemotherapeutic agent (1) has led to the development of other complexes of platinum, as well as complexes of ruthenium, which have similar substitution kinetics, but differ in biological reactivity and toxicities in vivo. (2-4) To date, there are no ruthenium-based anti-cancer drugs in routine clinical use, however imidazolium [*trans*-imidazoledimethylsulfoxide-tetrachlororuthenate (III)] (NAMI-A) and indazolium [*trans*-tetrachlorobis(1H-indazole) ruthenate(III)] (KP1109) have advanced to preclinical and/or clinical trials.(5-8) Most of the success to date with ruthenium based compounds has been with complexes bearing one or more labile ligands which, like cisplatin, allows the metal to directly bind with biological targets, particularly DNA. NAMI-A, KP1109, and the anti-tumor agents [*cis*-bis(acetonitrile)-1,10-phenanthroline-2-phenylpyridineruthenium(II)] hexafluorophosphate (RDC11) and ruthenium-aryl-X complexes(9, 10) all contain at least one labile ligand and it is postulated that these complexes directly bind biological targets upon loss of this ligand *in vivo*.

The biological activity of coordinately saturated ruthenium (II) polypyridyl complexes (RPC's), such as the trisphenanthroline complex (**1**$^{2+}$) (**Fig. 1**), was extensively studied by Dwyer and Schulman(11) in the 1950's and 60's and even prior to that by Beccari in the late 1930's.(12) These complexes differ from cisplatin and ruthenium complexes such as NAMI-A and KP1109 in that the ruthenium (II) ion lacks labile ligands and cannot directly form bonds with biological targets. Instead, early studies with radiolabeled [^{106}Ru(phen)$_3$]$^{2+}$ showed that the intact complex cation was the bioactive unit, that this complex was not metabolized in vivo and did not accumulate in any organ, and that nearly all the complex was recovered in the urine.(13) Despite this lack of reactivity in vivo, these RPC's were shown to possess biological activity both in vitro and in vivo.(13-16)

RPC **1**$^{2+}$ is modestly cytotoxic (IC$_{50}$ ~ 90 µM) with enhanced cytoxicity generally observed by increasing the lipophilicity of the complex.(17) The 3,4,7,8-tetramethyl-1,10-pheanthroline derivative of **1**$^{2+}$ was among the most cytotoxic of the derivatives found and was

3

shown to inhibit the growth of dispersed tumor cells (Landshultz ascites) in mice.(14) Since

these early studies, there have been numerous studies exploring the DNA-binding activity of

RPCs (18) and to a lesser extent the cytotoxicity of RPCs,(19-23) however, the anti-cancer

activity of these complexes in vivo has not been extensively studied. The paucity of follow up

studies is due, in part, to their observed neurotoxicity, as $\mathbf{1}^{2+}$ has been shown to be a

competitive inhibitor of acetyl cholinesterase (AChE) both in vitro and in vivo.(13, 24, 25) As a

consequence, the minimum lethal doses of $\mathbf{1}^{2+}$ (iodo salt) in mice is 12 μmol/kg when

administered by i.p. injection. A study of the peak ruthenium blood concentrations showed that

RPCs able to diffuse quickly through tissue and enter the bloodstream were more neurotoxic

than those slower to do so and that by increasing the complex lipophilicity it was possible to

ameliorate the neurotoxicity.(13) Interestingly, $\mathbf{1}^{2+}$ is non-toxic when administered orally.(11)

It has been possible to track the intracellular distribution of many of these RPC's due to

their inherent luminescence with both the nucleus and mitochondria often showing significant

accumulation.(19, 22, 26-28) As many RPCs have been shown to bind DNA, it is often

assumed that this is the biological target,(29) although the mitochondria(19, 25, 30) and the cell-

cell interface (20, 31) are also potential targets. In general, these RPCs bind to duplex DNA via

electrostatic and intercalative modes but usually they do not damage DNA unless an external

factor, such a light irradiation, is introduced.(32, 33)

We have shown that the dinuclear tatpp complex, [(phen)$_2$Ru(tatpp)Ru(phen)$_2$]Cl$_4$

([$\mathbf{4}$]Cl$_4$), (Fig. 1) is an effective DNA cleaving agent upon in situ reduction by glutathione (GSH)

and that the cleavage activity is potentiated upon lowering the oxygen concentration.(34) We

also demonstrated that the reduced forms of $\mathbf{4}^{4+}$ are competent for DNA cleavage under

anaerobic conditions without GSH present. Under identical reducing conditions, the closely

related RPCs $\mathbf{1}^{2+}$, [(phen)$_2$Ru(dppz)]$^{2+}$ and [(phen)$_2$Ru(tpphz)Ru(phen)$_2$]$^{4+}$ ($\mathbf{2}^{4+}$)(see Figure 1 for

the structures of dppz, tpphz, and $\mathbf{2}^{4+}$) are neither reduced nor do they exhibit any DNA

cleavage activity. We postulated that the redox-activity of the RPC, $\mathbf{4}^{4+}$, was responsible for the

4

DNA cleavage activity and that the cleavage activity may be useful therapeutically. Moreover,
the inverse sensitivity to the dioxygen concentration could enhance the cleavage activity in
hypoxic tumors. Finally, we reasoned that the increased size and lipophilicity of 4^{4+} and the
related mononuclear complex, [(phen)$_2$Ru(tatpp)]Cl$_2$ (3^{2+}) may ameliorate any neurotoxic side
effects of these complexes in vivo.   Herein, we evaluate 3^{2+} and 4^{4+} as potential anti-cancer
agents in a pre-clinical study.

MATERIALS AND METHODS

Abbreviations, Stereochemistry, and Nomenclature

The ruthenium complexes, [**1**]Cl$_2$, [**2**]Cl$_4$, [**3**]Cl$_2$, and [**4**]Cl$_4$, are all water soluble salts composed
of the complex cations, $\mathbf{1}^{2+}$, $\mathbf{2}^{4+}$, $\mathbf{3}^{2+}$, and $\mathbf{4}^{4+}$ and chloride anions. These complex cations,
collectively identified as RPCs, are composed of Ru(II) ions bound to 1,10-phenanthroline
(phen), tpphz, and/or (tatpp) polypyridyl ligands (**Fig. 1**). If the counterion is not explicitly listed,
it can be assumed to be chloride. All of the complexes are chiral (Δ or Λ) due to the three-fold
helical chirality at the ruthenium centers where the descriptor Δ or Λ is used to indicate right or
left-handed chirality, respectively, at the ruthenium centers. Typically, these complex cations
are isolated as a racemic mixture for the monomers ($\mathbf{1}^{2+}$ and $\mathbf{3}^{2+}$) or as diastereotopic mixtures
($\Delta\Delta$, $\Lambda\Lambda$ and $\Delta\Lambda$) for the dinuclear complex ($\mathbf{2}^{4+}$ and $\mathbf{4}^{4+}$). The complex cations are chemically
robust and stable to decomposition and racemization in aqueous solution over extended periods
of time (i.e. months). Because of this stability, it is possible to prepare and isolate these
complexes in diastereomerically and enantiomerically pure forms, i.e., Δ-$\mathbf{1}^{2+}$ and Λ-$\mathbf{1}^{2+}$, Δ-$\mathbf{3}^{2+}$
and Λ-$\mathbf{3}^{2+}$, $\Delta\Delta$-$\mathbf{4}^{4+}$, $\Lambda\Lambda$-$\mathbf{4}^{4+}$ and $\Delta\Lambda$-$\mathbf{4}^{4+}$.   In the following studies, we typically used the racemic
or diastereotopic mixture initially, and only used enantiopure substances where specifically
indicated with the appropriate chiral descriptor. If no descriptor is given, then the racemate was
used for $\mathbf{1}^{2+}$ and $\mathbf{3}^{2+}$ and the diastereotopic mixture was used for $\mathbf{2}^{4+}$ and $\mathbf{4}^{4+}$.

5

Reagents

Reagents for cell culture were purchased from Life Sciences Technologies, Inc., Grand Island, NY. Supercoiled plasmid pUC 18 DNA was purchased from Bayou Biolabs, New England. Agarose, ethidium bromide, glutathione (GSH), dimethyl sulfoxide (DMSO), 2,2,6,6-tetramethylpiperidine-1-oxyl (TEMPO), trizma base and horseradish peroxidase (HRP)-conjugated secondary antibodies were from Sigma Aldrich. Fluorescein terminal deoxynucleotidyl transferase (TdT)–mediated dUTP nick end labeling (TUNEL) apoptosis assay kit was from Promega (Madison, WI). pAkt (S^{473}) antibody was procured from Upstate Cell Signaling (Lake Placid, NY). pPI3K (Y^{458}), pEGFR (Y^{1068}), and cleaved PARP antibodies were from Cell Signaling Technologies (Danvers, MA).   Antibodies against Bcl2, Bax, cdk4, cyclin B1, pRb (S^{780}), caspase, and GAPDH were obtained from Santa Cruz Biotechnology (Columbus, OH). CasPACE FITC-VAD-FMK in situ marker, apoptosis detection system was purchased from Promega Inc. (Madison, WI). Mounting medium Fluro-gel II containing DAPI was procured from Electron Microscopy Sciences, (Hatfield, PA, USA). The complexes, [**1**]Cl$_2$(35) [**2**]Cl$_4$(36) [(phen)$_2$Ru(tpphz)]Cl$_2$(36, 37), [**3**]Cl$_2$ (38), [**4**]Cl$_4$ (39), and select enantiomers, Δ-**1**$^{2+}$ and Λ-**1**$^{2+}$,(35) Δ-**3**$^{2+}$ and Λ-**3**$^{2+}$,(38) and diastereomers, $\Delta\Delta$-**3**$^{4+}$, $\Lambda\Lambda$-**3**$^{4+}$ and $\Delta\Lambda$-**3**$^{4+}$,(40) were prepared previously described. Enantiopurity was ascertained using chiral HPLC as described in ref (35) and was 97% or greater for all complexes.

DNA Cleavage Assay

DNA cleavage was carried out as previously described.(34) Briefly, RPC was added to a reaction mixture containing 7 mM sodium phosphate (pH 7.0) and pUC18 DNA (0.1 μg/μL). The reaction was quenched by addition of 2 μL sodium acetate (pH 5.2) and 80 μL ethanol and

6

incubated at –20 ^{o}C to complete precipitation. The DNA was pelleted, air-dried, resuspended in

15 mM Tris-HCl pH 8.0, 0.3 mM EDTA, 3% glycerol and 0.1% w/v bromophenol blue, and

subjected to horizontal slab agarose (1%) gel at 80 V for 90 min with the gel immersed in

TAE/0.2 mM ethidium bromide (0.2 mM). Results were visualized and recorded by using a

UVPGDS 8000 gel analysis system. For studies under anaerobic conditions, all reagent

solutions were degassed using N_2. DNA stock was degassed using five freeze-pump-thaw

cycles under N_2. Degassed reagents were taken into a N_2 glove box and all the solutions were

prepared inside it to minimize further contamination with oxygen. DMSO and TEMPO were

added inside the glove box where the assays were completed and reactions quenched by

precipitating the DNA using 2 μL of degassed sodium acetate at pH 5.2 and 80 μL degassed

ethanol under N_2.

Cell Lines and Cultures

Human non small cell lung cancer (NSCLC) cell lines H358 (bronchioalveolar), H226

(squamous cell carcinoma), human aortic vascular smooth muscle cells (HAVSMC), and human

umbilical vascular endothelial cells (HUVEC) were obtained and maintained as previously

described.(41)

Cytotoxicity Assays

Cell viability and density was measured by counting trypan-blue dye excluding cells in a

hemocytometer, and 2 X 10^4 viable cells in respective full culture media were placed into each

well of a 96-well plate and allowed to grow at 37 ^{o}C for 24 h prior to addition of RPCs. After 96-

h incubation, MTT assay was carried out as previously described.(41)   Both Δ-[**3**]Cl$_2$ and $\Delta\Delta$-

[**4**]Cl$_4$ were accepted by the Developmental Therapeutics Program (DTP) of the NCI for the NCI-

60 cell line one-dose screen and were assigned registration numbers NSC 747949 and

7

747950, respectively. Only [Δ-**3**]Cl$_2$ (NSC 747949) had sufficient activity in the single dose screen to proceed to the 5 dose screen. However, because the NCI-60 screen is not done under hypoxic conditions, thus may not truly reflect in-vivo activity, we included ΔΔ-[**4**]Cl$_4$ in present studies.

Non-Hypoxic/Hypoxic cytotoxicity. H358 cells were plated in 60mm x 15mm cell dishes with equal cell densities respectively. 10 dishes were used per compound being tested; 5 dishes for normoxic and 5 dishes for hypoxic. Before assay each 5 set dishes were washed with PBS and media changed with 3 ml aliquot of compound solution and put into incubators (normoxic was monitored at 5% CO$_2$ and 18% O$_2$ and hypoxic was monitored at 5% CO$_2$ and 1% O$_2$) accordingly. Cells were left in both incubator conditions for 24 h and every 4 h cells were checked for viability. Cytotoxicity of cells was determined by cell count with hemocytometer w/ Trypan blue staining.

In situ **caspase-3 assay for Apoptosis** Normal (HUVEC) and lung cancer (H358) cells (0.1x10^6) were plated on glass cover slip in tissue culture treated 12 well plates and incubated with either 10 μM of Δ-**3**$^{2+}$ or ΔΔ-**4**$^{4+}$ for 12 h at 37 °C. Apoptotic cells were detected by staining with 5 μM Caspase FITC-VAD-FMK (Promega) *in situ* marker for 30 min in the dark. The slides were rinsed with PBS and fixed with 4% paraformaldehyde for 30 min, and mounted in a medium containing DAPI (1.5 μg/ml). Images were taken on Olympus Provis AX70 fluorescence microscope. Photographs taken at identical exposure at 40 x magnification are presented.

Effect of Ru-compounds on apoptosis by TUNEL assay Normal (HUVEC) and lung cancer (H358) cells were grown on cover-slips. For Ru-compounds treatment, cells were

8

incubated with 10 µM either Δ-3^{2+} or $\Delta\Delta$-4^{4+} before TUNEL assay using Promega fluorescence detection kit according to the protocol provided by the manufacturer. Slides were analyzed by fluorescence microscope (Olympus Provis AX70). Photographs taken at identical exposure at 40 x magnification are presented. Apoptotic cells showed green fluorescence.

Animal Studies

All animal experiments were carried out in accordance with a protocol approved by the Institutional Animal Care and Use Committee. Hsd: Athymic nude nu/nu mice were obtained from Harlan, Indianapolis, IN. C57 BL/6 mice were obtained from Harlan (Indianapolis, Indiana). The maximum tolerable dose (MTD, mg complex/kg mouse) was determined in 10 weeks old male mice (3 per group) treated with 100 µL (i.p. injection) of RPC at 6 concentrations ranging from 1 to 50 mg/mL. MTD was defined as the dose level causing no deaths. For lung cancer xenograft studies, H358 NSCLC cells (1 X 10^6/ µL PBS) were injected into the flanks of 10 wk *nu/nu* mice, Harlan (Indianapolis, Indiana), followed 14 days later by i.p. injection of RPC in 100 µL PBS. Animals were examined daily for signs of distress and tumors were measured in two dimensions using Vernier calipers.(42) For statistical analysis, the mean tumor volume data versus time for the two RPC treated groups were combined to a single group with n = 6 and a control group. A repeated measures ANOVA analysis of the treated and control group data was obtained using the SAS ® programmer PROC MIXED program.

RESULTS

Cytotoxicity

The IC_{50} data from initial screening studies of antineoplastic activity of a series of RPCs were performed in two NSCLC cell lines, H358 and H226 (**Table 1**). The tatpp containing complexes 3^{2+} and 4^{4+} were significantly more cytotoxic (IC_{50}s ~12-16 µM) than the tpphz complexes, 2^{4+}

9

and [(phen)$_2$Ru(tpphz)]$^{4+}$ (~45 μM), or the homoleptic complexes phen **1**$^{2+}$ (90 μM) and

[Ru(bpy)$_3$]$^{2+}$ (200 μM) for both cell lines. Stereoisomers with the Δ configuration were more

cytotoxic than those with the Λ configuration. The $\Delta\Delta$ enantiomer of **4**$^{4+}$ and the Δ enantiomer

for **3**$^{2+}$ were the most cytotoxic with IC$_{50}$ values approximately one-half that of their mirror

images. The IC$_{50}$ value for racemic **3**$^{2+}$ falls between the values of the two enantiomers

suggesting that the toxicity of the racemate is simply the average of the two enantiomers. For

the stereochemically more complicated dimers, the mixture of $\Delta\Delta$-**4**$^{4+}$, $\Lambda\Lambda$-**4**$^{4+}$, and $\Delta\Lambda$-**4**$^{4+}$ (*mix*-

4^{4+}), the IC$_{50}$ also appears to be a weighted average of the IC$_{50}$'s for individual diastereomers.

Interestingly, the IC$_{50}$ for *meso*-diastereomer, $\Delta\Lambda$-**4**$^{4+}$, was not significantly different from the

$\Lambda\Lambda$–diastereomer, indicating that both chiral centers must be Δ to achieve a significant biological

effect.

As shown in Figure 2A, the cytotoxicity of Δ-**3**$^{2+}$ is enhanced when the H358 cells were

incubated under hypoxic conditions (1 %O$_2$) relative to normoxic conditions. This figure also

includes the data from two controls, cisplatin and [Ru(phen)$_2$(dppz)]$^{2+}$, neither of which showed

significant potentiation under hypoxic conditions as expected. Significantly, Δ-**3**$^{2+}$ and $\Delta\Delta$-**4**$^{4+}$

are significantly more cytotoxic towards malignant cell lines as the IC$_{50}$'s for normal HUVEC and

HUVSMC cells are around 100 μM, an approximate 10-fold difference in cytotoxicity. This

selectivity is also observed in the Caspase-3 and TUNEL assays, (Fig. 2C) and appears to be

unique to the tatpp-based complexes. Dwyer and co-workers found little selectivity in the

cytotoxicity of RPCs such as **1**$^{2+}$ or its tetramethylphenanthroline derivative towards malignant,

adult, embryonic, epithielial, and fibroblastic cells.(11)

DNA Cleavage by Δ-3^{2+} and $\Delta\Delta$-4^{4+} under aerobic and anaerobic conditions

Since the above studies indicated that Δ-**3**$^{2+}$ and $\Delta\Delta$-**4**$^{4+}$ were the most active

compounds, sufficient amounts of these were synthesized, purified, and authenticated for

10

further studies. We have previously shown that the reduced form of the di-ruthenium compound

4^{4+} shows hypoxia sensitive DNA cleavage and that this reduced complex is readily formed via

addition of common agents such GSH or ascorbic acid.(34) The data presented here in Figure

2 confirmed similar activity of the mono-ruthenium complex, Δ-3^{2+}. Supercoiled plasmid DNA

was incubated with Δ-3^{2+} and $\Delta\Delta$-4^{4+} in the presence or absence of GSH and O_2. In this assay,

the conversion of supercoiled plasmid DNA to the circular form is used to monitor single-strand

cleavage events using agarose gel electrophoresis. As can be seen in Figure 3A, RPCs Δ-3^{2+}

and $\Delta\Delta$-4^{4+} only show DNA cleavage when GSH is present (lanes 4, 5, 7, 8) and this cleavage is

appreciably enhanced when O_2 is absent (lanes 5 and 8, respectively). As shown in Figure 3B,

RPC Δ-3^{2+} was also incubated with DNA in the presence of GSH and the oxygen radical

scavenger DMSO (43) and the carbon and metal centered radical scavenger TEMPO (43)

under anaerobic conditions. As seen in Lane 4 (Fig 3B) there is an extensive amount of DNA

cleavage upon treatnment with Δ-3^{2+} and GSH under anerobic conditions. Addition of DMSO

did not affect this cleavage activity (lane 6) whereas addition of TEMPO (lane 5) appreciably

attenuated the cleavage, supporting a carbon-based radical intermediate, and ruling out any

significant role for reactive oxygen species. The activity is indeed unique in comparison with

transition metal-mediated DNA cleavage by cisplatin, which is inhibited by GSH.(44) Having

demonstrated DNA-cleaving activity, both compounds were submitted to the DTP for NCI-60

panel screening.

Spectrum of Activity and Predicted Mechanism of Action

The NCI-60 panel single dose cytotoxicity (10 μM) screen for compounds Δ-3^{2+} and $\Delta\Delta$-

4^{4+} performed by the DTP revealed that RPC Δ-3^{2+} is more cytotoxic than $\Delta\Delta$-4^{4+} (mean growth

percentages of 42 % and 80 %, respectively for the whole panel). RPC Δ-3^{2+} was subsequently

selected for the 5-dose screen.   RPC Δ-3^{2+} showed some its best activity against leukemia,

11

colon cancer, lung cancer and melanoma cell lines. Interestingly, the 5-dose assay predicted a

unique and complex mechanism (**Table 2**), a cross between the antimitotic agent paclitaxel

(corr. 0.909), the RNA/DNA antimetabolite pyrazofurin (corr. 0.666), the Topo II inhibitor,

dibenzyldaunomycin (corr. 0.515) and multiple alkylating agents (corr. 0.4 – 0.5). It is useful to

note that there are no alkylating moieties in the complex and no chemical evidence of its

behavior as an alkylating agent. These observations are consistent flow-cytometry studies

showing a marked G2-M block (see Fig. 2B). Similar degree of specific G2-block was seen with

paclitaxel, an agent that does not directly cause DNA-fragmentation, but does activate intrinsic

apoptosis through bcl2. Some similarity in mechanism to other tubulin-binding drugs that also

activate bcl2 agents that cause single (most alkylating agents) or double-stranded DNA breaks

(radiation, intercalating agents) also typically cause G2 arrest.   These findings concur with the

known subcellular localization of these compounds in the nucleus and mitochondria, and with

previous studies of RPC **3**$^{2+}$ and **4**$^{4+}$ that binds DNA tightly ($K_b \sim 10^8$ M^{-1}, *in vitro*) via an

intercalative mode, (45, 46) typical for RPCs with large planar aromatic rings.(18) Indeed,

analysis of the whole cell (wc) and nuclear fractions (nf) of RPC treated (5 μM) H-358 cells for

uptake of ruthenium by graphite furnace atomic absorption spectroscopy, a showed early

concentration spikes in the nf. After 1 h incubation, cells revealed [Ru] of ~7 μg RPC/mg wc

and ~27 μg RPC/mg nf for both Δ-**3**$^{2+}$ and ΔΔ-**4**$^{4+}$. The ruthenium concentration in the whole

cells and nucleus level off and were essentially equal at 30 μg RPC/mg for Δ-**3**$^{2+}$ and 18 μg

RPC/mg for ΔΔ-**4**$^{4+}$ after 24 h and remain this way for 72 h.

Spectrum of Activity and Mechanism of Cell Death

The activity predicted by the NCI-60 panel towards NSCLC was confirmed in further

studies showing significant activity in NSCLC (see Fig. 2). Cell-cycle analysis indicated that

RPC Δ-**3**$^{2+}$ caused a profound G2 block, characteristic of DNA fragmenting agents such as

12

radiation and anthracyclines, but also paclitaxel, which does not directly cause DNA fragmentation. Caspase-3 activation, PARP-cleavage, and TUNEL positivity in IHC was observed upon treatment of H358 with RPCs confirming an increase in the percentage of cells in early and late apoptosis. In contrast, similar treatment of HUVEC or HUVSMC cells with RPCs Δ-3^{2+} or $\Delta\Delta$-4^{4+} did not show apoptosis, consistent with the lesser degree of cytotoxicity observed against these cell lines. Simultaneous cytochrome-c release and caspase-8 activation in H358 cells indicated that both intrinsic and extrinsic pathways are activated. Treatment with either Δ-3^{2+} or $\Delta\Delta$-4^{4+} caused a generalized decrease in kinase signaling (Fig. 2D), with reduction in pAKT, pEGFR, PI3K, pRb, CDK4, cyclinB1, and bcl2. Bax was significantly increased by $\Delta\Delta$-4^{4+}, but less so by Δ-3^{2+}, perhaps a reason for its greater efficacy.

Animal Toxicity in Mouse

MTD determinations were performed with 1^{2+}, 2^{4+}, 3^{2+}, 4^{4+}, and the individual stereoisomers of 4^{4+}. As seen in **Table 3**, it was clear that the compounds containing the tatpp ligand, 3^{2+} and 4^{4+}, were significantly less toxic relative to the others, with the tetracationic complex 2^{4+} exhibiting the greatest cytotoxicity.   The single ruthenium-tatpp complex 3^{2+} (MTD 65 μmol/Kg), was the least toxic but comparable with the MTD found for the diastereotopic mixture of the di-ruthenium complex 4^{4+} (MTD 43 μmol/Kg), it was equitoxic with the $\Delta\Delta$-4^{4+} enantiomer (64 μmol/Kg). Interestingly, the toxicity does not seem to correlate with the complex overall charge or size. Complexes 2^{4+} and 4^{4+} differ little in charge or size, but exhibit significantly different toxicities (MTD 2.5 *vs.* 43 μmol/Kg, respectively).   Among the stereoisomers of 4^{4+}, the $\Delta\Delta$-enantiomer exhibited the least cytotoxicity and was equitoxic with 3^{2+}. From these data and the cytotoxcity studies, It is clear that there is some benefit in working with $\Delta\Delta$-4^{4+} and Δ-3^{2+} both in terms of efficacy and in lessened animal toxicity, which is

13

consistent with earlier studies on Δ-$\mathbf{1}^{2+}$ and Λ-$\mathbf{1}^{2+}$.(13) Mice receiving lethal doses were observed to display lethargy, hind-limb paralysis, and respiratory distress shortly after ip injection. These symptoms are associated with neurotoxicity which has been reported in earlier studies of $\mathbf{1}^{2+}$.(13) Mice showing no abnormal symptoms 15 min after ip injection were generally fine thereafter.

Growth Inhibition of H358 NSCLC in a Nude Mouse Xenograft Model

Tumor-bearing animals with established *s.c.* implanted H358 tumors ~40 mm^2 were treated on days 0, 15, and 30 by *i.p.* injection containing 1 mg (~50% of MTD) RPC (Δ-$\mathbf{3}$Cl$_2$ or $\Delta\Delta$-$\mathbf{4}$Cl$_4$) in 100 μL PBS or PBS alone. As seen in Figure 4, rapid and near linear growth in tumor volume was seen in the control group. The treated groups initially showed similar tumor growth to the control but after day 6, tumor growth slowed and only gradually increased over the remaining course of the experiment. Notably, the two treated groups show nearly identical behavior with the Δ-$\mathbf{3}^{2+}$ treated group showing slightly less tumor growth than the $\Delta\Delta$-$\mathbf{4}^{4+}$ group. For statistical purposes, the two treated groups were combined (n = 6) and using a mixed linear model to fit the data, the equality of the group means was tested using a repeated measures ANOVA analysis. Results indicate that the main group effect, the main time effect, and their interaction term are all very significant (P-values <0.00001).   If we consider the divergence of the combined treated (n = 6) and control (n = 3) groups by day 14, one day before the second drug dose was administered, the MTV of the treated group is 35 % that of the control group. By 32 days, all control animals had died or were sacrificed for tumors > 150 mm^2. Tumors in the treated group were only 20 % the size of the control group at that time (P <0.0001). The last treatment was given on day 30 and, as can be seen in Figure 4, no further tumor growth was seen in either individual treated group over the next 30 day period. Survival was also improved, with 0 alive at 32 days for control, 2/3 and 2/3 alive at 60 days with both Δ-$\mathbf{4}^{2+}$ and $\Delta\Delta$-$\mathbf{3}^{4+}$,

14

respectively. Ruthenium treated mice had weight gain comparable to non-tumor bearing

controls (Fig. 4).

15

DISCUSSION

These studies are the first demonstration of *in-vivo* anti-cancer activity of systemically administered RPCs (lacking labile ligands) in NSCLC. It is clear that RPC's containing the tatpp ligand (3^{2+} and 4^{4+}) outperform the other RPCs (1^{2+}, 2^{4+}, [Ru(phen)$_2$(dppz)]$^{2+}$ and [Ru(phen)$_2$(tpphz)]$^{2+}$) in terms of efficacy and selectivity for inducing apoptosis in cultured NSCLC cell lines, causing a specific G2M arrest, and triggering apoptosis through both intrinsic and extrinsic pathways. Most significantly, they demonstrate statistically significant tumor growth repression ($P < 0.0001$) in vivo and a doubling of survival time, as shown in Figure 4.

By far, the most important feature discovered was the enhanced biological activity associated with use of tatpp ligand (found only in RPC's 3^{2+} and 4^{4+}). Although tatpp is insoluble alone, coordination to Ru(II) leads to stable, soluble complexes, like 3^{2+} and 4^{4+}, in which tatpp-based reductive processes are observed at potentials positive of -0.25 V (vs. NHE at pH 7.0)(47, 48). In contrast, most RPC's like 1^{2+} and 2^{4+} are significantly harder to reduce and usually require reduction potentials negative of -0.70 V or more.(18, 33) This low reduction potential means that RPCs are readily reduced by common cellular reductants, and we have shown that these reductions are centered on the tatpp ligand, not the Ru(II) ion, with concomitant formation of a carbon radical species. Because RPCs 3^{2+} and 4^{4+} as well as related complexes 2^{4+}, [Ru(phen)$_2$(dppz)]$^{2+}$, and [Ru(phen)$_2$(tpphz)]$^{2+}$, are known to bind DNA via intercalation,(18) the tatpp carbon radical in the reduced species is in intimate contact with the DNA. We hypothesize that H atom abstraction from the deoxyribose unit as the likely mechanism of DNA damage. Dioxygen can react with this radical species to reform the tatpp complex(47) and in this manner attenuate the DNA cleavage process. As the tatpp complex can be reduced again, the steady-state concentration of the key carbon-radical species is dependent on the local concentrations of O$_2$ and cellular reducing agents. Ruthenium atomic

16

absorption analysis shows ruthenium in the nuclear fractions of whole H358 cells incubated with

Δ-3^{2+} and $\Delta\Delta$-4^{4+}, indicating that the RPC are making it to the nucleus. The enhanced

cytotoxicity seen for Δ-3^{2+} in treated H358 cells under hypoxia (Fig 2A.) suggests this carbon-

radical mediated cleavage mechanism is active in live cells and potentially in vivo.

RPCs 3^{2+} and 4^{4+} show good selectivity for malignant cells and one possible explanation

is that these RPCs exhibit different transport mechanisms in cells compared to the simpler

RPCs, such as 1^{2+}, 2^{4+}, and $[(phen)_2Ru(dppz)]^{2+}$, which are generally shown to enter cells via

passive diffusion.(27, 28) Recently, Thomas and coworkers showed that the structurally related

tpphz dimers, 2^{4+} and $[(bpy)_2Ru(tpphz)Ru(bpy)_2]^{4+}$ are actively transported into MCF-7 cells in a

non-endocytotic but temperature-dependent manner.(22)   If 3^{2+} and 4^{4+} similarly undergo active

transport, the differences in the transport pathways in malignant cells versus normal cells could

explain the selectivity. Not only are the tpphz dimers actively transported, they were also

observed to localize in the nucleus as demonstrated by fluorescence and co-localization with

another nuclear stain, DAPI. Complexes 3^{2+} and 4^{4+} are not luminescent but given the observed

detection of ruthenium in the nucleus and the similarity of their structure to

$[(bpy)_2Ru(tpphz)Ru(bpy)_2]^{4+}$, it is reasonable that they exhibit the same transport and

localization properties as the tpphz RPCs.(22) The important difference between these two

classes of RPCs (tatpp- vs tpphz-based RPCs) is that the latter are not easily reduced, do not

show any DNA cleavage activity, and are considerably less cytotoxic which only further

emphasizes the importance and role of the redox-active ligand in the observed biological

activity.

The analysis of the cytotoxicity of Δ-3^{2+} and $\Delta\Delta$-4^{4+} (NSC 747949 and 747950,

respectively) in the NCI-60 panel revealed unique patterns of cytotoxicity and the former had

sufficient activity to proceed to multidose screening. The predicted mechanism of action by the

NCI panel was found to be consistent with the known nucleotide and mitochondrial binding

17

activity and DNA cleaving activity of this compound. Because an anaerobic environment is not utilized in the NCI-60 panel, mechanism of action is incompletely assessed, however, our cytotoxicity studies under hypoxic conditions reveal enhanced activity for Δ-**3**$^{2+}$ in H358 cells relative to those under normoxic conditions (Fig. 2A). It is clear that these molecules bind DNA and mitochondria (19, 25, 30) strongly, cleave DNA, cause a specific G2M arrest, and trigger apoptosis through both intrinsic and extrinsic pathways. Another possibility is the involvement of receptor-mediated death pathways where the tumor factor necrosis (TNF) family of death receptors activate the initiator caspase-8 which can activate caspase-3 without involve the mitochondrial-mediated apoptosis.

In summary, we have systematically optimized structural features of RPCs, selecting features that optimize cancer-selective apoptosis in cultured NSCLC cell lines and on the basis of animal toxicity, and have demonstrated unique chemical mechanism of reductive DNA cleavage through a carbon-centered radical mechanism. Due to the ease with which the tatpp ligand can be reduced in situ, RPCs **3**$^{2+}$ and **4**$^{4+}$, display a unique and potentially hypoxia-selective ability to bind and cleave DNA through a carbon-centered radical mechanism. Combined these data show that RPCs, and specifically RPCs with bioreducible ligands, represent a pharmacologically favorable class of compounds with a natural selectivity for cancer cells and promising hypoxia selective activity.

18

REFERENCES

1.   Lippert B, Editor. Cisplatin Chemistry and Biochemistry of a Leading Anticancer Drug. Weinheim: Wiler-VCH; 1999.

2.   Clarke MJ. Ruthenium metallopharmaceuticals. Coord Chem Rev 2003; 236: 209-33.

3.   Jakupec MA, Galanski M, Arion VB, Hartinger CG, Keppler BK. Antitumour metal compounds: more than theme and variations. Dalton Transactions 2008:183-94.

4.   Allardyce CS, Dyson PJ. Ruthenium in medicine: Current clinical uses and future prospects. Platinum Metals Review 2001; 45: 62-9.

5.   Bergamo A, Gava B, Alessio E, Mestroni G, Serli B, Cocchietto M, et. al. Ruthenium-based NAMI-A type complexes with in vivo selective metastasis reduction and in vitro invasion inhibition unrelated to cell cytotoxicity. Int J Oncol 2002; 21: 1331-8.

6.   Depenbrock H, Schmelcher S, Peter R, Keppler BK, Weirich G, Block T, et al. Preclinical activity of trans-indazolium [tetrachlorobisindazoleruthenate(III)] (NSC 666158; IndCR; KP 1019) against tumour colony-forming units and haematopoietic progenitor cells. European Journal of Cancer 1997; 33: 2404-10.

7.   Lentz F, Drescher A, Lindauer A, Henke M, Hilger RA, Hartinger CG, et al. Pharmacokinetics of a novel anticancer ruthenium complex (KP1019, FFC14A) in a phase I dose-escalation study. Anti-Cancer Drugs 2009; 20: 97-103.

8.   Hartinger CG, Jakupec MA, Zorbas-Seifried S, Groessl M, Egger A, Berger W, et al. KP1019, A New Redox-Active Anticancer Agent – Preclinical Development and Results of a Clinical Phase I Study in Tumor Patients. Chemistry & Biodiversity 2008; 5: 2140-55.

9.   Morris RE, Aird RE, Murdoch PdS, Chen H, Cummings J, Hughes ND, et al. Inhibition of Cancer Cell Growth by Ruthenium(II) Arene Complexes. J Med Chem 2001; 44: 3616-21.

19

10.   Meng X, Leyva ML, Jenny M, Gross I, Benosman S, Fricker B, et al. A Ruthenium-Containing Organometallic Compound Reduces Tumor Growth through Induction of the Endoplasmic Reticulum Stress Gene CHOP. Cancer Research 2009; 69: 5458-66.

11.   Shulman A, Dwyer FP. Metal Chelates in Biological Systems. In: Dwyer FP, Mellor DP, editors. Chelating Agents and Metal Chelates. New York: Academic Press; 1964. p. 383-439.

12.   Beccari E. Pharmacological studies on the ferrous tri-2,2'-bipyridyl complex. IV. Relation between concentration in the blood and action on the central nervous system. Boll - Soc Ital Biol Sper 1941; 16: 216-18.

13.   Koch JH, Rogers WP, Dwyer FP, Gyarfas EC. The metabolic fate of tris-1,10-phenanthroline ruthenium-106 (II) perchlorate, a compound with anticholinesterase and curare-like activity. Australian J Biol Sci 1957; 10: 342-50.

14.   Dwyer FP, Mayhew E, Roe EMF, Shulman A. Inhibition of Landschuetz ascites tumor growth by metal chelates derived from 3,4,7,8 - tetramethyl - 1,10 - phenanthroline. Br J Cancer 1965; 19: 195-9.

15.   Koch JH, Gyarfas EC, Dwyer FP. Biological activity of complexions. Mechanism of inhibition of acetylcholinesterase. Aust J Biol Sci 1956; 9: 371-81.

16.   Dwyer FP, Gyarfas EC, Rogers WP, Koch JH. Biological activity of complex ions. Nature (London, U K) 1952; 170: 190-1.

17.   White DO, Harris AW, Cheyne IM, Shew M. Actions of metal chelates of substituted 1,10-phenanthrolines on viruses and cells. 3. Actions on cultured cells. Austral J Exp Biol Med Sci 1969; 47: 81-9.

18.   Augustyn KE, Pierre VC, Barton JK, Editors. Metallointercalators as probes of DNA recognition and reactions. Wiley Encyclopedia of Chemical Biology. 2009: John Wiley & Sons, Inc.

20

19.   Pisani MJ, Weber DK, Heimann K, Collins JG, Keene FR. Selective mitochondrial accumulation of cytotoxic dinuclear polypyridyl ruthenium(II) complexes. Metallomics 2010; 2: 393-6.

20.   Schatzschneider U, Niesel J, Ott I, Gust R, Alborzinia H, Wölfl S. Cellular Uptake, Cytotoxicity, and Metabolic Profiling of Human Cancer Cells Treated with Ruthenium(II) Polypyridyl Complexes [Ru(bpy)$_2$(N-N)]Cl$_2$ with N-N=bpy, phen, dpq, dppz, and dppn. ChemMedChem 2008; 3: 1104-9.

21.   Pascu G, Hotze A, Sanchez-Cano C, Kariuki B, Hannon M. Dinuclear Ruthenium(II) Triple-Stranded Helicates: Luminescent Supramolecular Cylinders That Bind and Coil DNA and Exhibit Activity against Cancer Cell Lines. Angew Chem Int Ed 2007; 46: 4374-8.

22.   Gill MR, Garcia-Lara J, Foster SJ, Smythe C, Battaglia G, Thomas JA. A ruthenium(II) polypyridyl complex for direct imaging of DNA structure in living cells. Nat Chem 2009; 1: 662-7.

23.   Novakova O, Kasparkova J, Vrana O, van Vliet PM, Reedijk J, Brabec V. Correlation between Cytotoxicity and DNA Binding of Polypyridyl Ruthenium Complexes. Biochemistry 1995; 34: 12369-78.

24.   Dwyer FP, Gyarfas EC, Wright RD, Shulman A. Effect of inorganic complex ions on transmission at a neuromuscular junction. Nature 1957; 179: 425-6.

25.   Koch JH, Gallagher CH. Effect of Some Neuromuscular Blocking Agents on Mitochondrial Enzyme Systems. Nature 1959; 184: 1039-41.

26.   Mayhew E, Roe EM, Shulman A. Microscopical observations on the effects of phenanthroline chelates on Landschütz ascites tumour cells. J R Microsc Soc 1965; 84: 475 - 83.

27.   Puckett CA, Barton JK. Methods to Explore Cellular Uptake of Ruthenium Complexes. J Am Chem Soc 2007; 129: 46-7.

28.   Puckett CA, Barton JK. Mechanism of Cellular Uptake of a Ruthenium Polypyridyl Complex. Biochemistry 2008; 47: 11711-6.

21

29.   Brabec V, Novakova O. DNA binding mode of ruthenium complexes and relationship to tumor cell toxicity. Drug Resist Updates 2006; 9: 111-22.

30.   Tan C, Lai S, Wu S, Hu S, Zhou L, Chen Y, et al. Nuclear Permeable Ruthenium(II) β-Carboline Complexes Induce Autophagy To Antagonize Mitochondrial-Mediated Apoptosis. J Med Chem 2010; 53: 7613-24.

31.   Zava O, Zakeeruddin SM, Danelon C, Vogel H, Gratzel M, Dyson PJ. A Cytotoxic Ruthenium Tris(Bipyridyl) Complex that Accumulates at Plasma Membranes. ChemBioChem 2009; 10: 1796-800.

32.   Sun Y, Joyce LE, Dickson NM, Turro C. Efficient DNA photocleavage by [Ru(bpy)$_2$(dppn)]$^{2+}$ with visible light. Chem Commun 2010; 46: 2426-8.

33.   Moucheron C, De MAK, Kelly JM. Photophysics and photochemistry of metal polypyridyl and related complexes with nucleic acids. Struct Bonding (Berlin) 1998; 92: 163-216.

34.   Janaratne TK, Yadav A, Ongeri F, MacDonnell FM. Preferential DNA Cleavage under Anaerobic Conditions by a DNA-Binding Ruthenium Dimer. Inorg Chem 2007; 46: 3420-2.

35.   Sun P, Krishnan A, Yadav A, Singh S, MacDonnell FM, Armstrong DW. Enantiomeric Separations of Ruthenium(II) Polypyridyl Complexes Using High-Performance Liquid Chromatography (HPLC) with Cyclodextrin Chiral Stationary Phases (CSPs). Inorg Chem 2007; 46: 10312-20.

36.   MacDonnell FM, Bodige S. Efficient Stereospecific Syntheses of Chiral Ruthenium Dimers. Inorg Chem 1996; 35: 5758-9.

37.   Bolger J, Gourdon A, Ishow E, Launay J-P. Mononuclear and Binuclear Tetrapyrido[3,2-a:2',3'-c:3'',2''-h:2''',3'''-j]phenazine (tpphz) Ruthenium and Osmium Complexes. Inorg Chem 1996; 35: 2937-44.

38.   Wärnmark K, Thomas JA, Heyke O, Lehn J-M. Stereoisomerically Controlled Inorganic Architectures: Synthesis of Enantio- and Diastereo-merically Pure Ruthenium-Palladium Molecular Rods from Enantiopure Building Blocks. Chem Commun 1996: 701-2.

22

39.   Kim M-J, Konduri R, Ye H, MacDonnell FM, Puntoriero F, Serroni S, et al. Dinuclear ruthenium(II) polypyridyl complexes containing large, redox-active, aromatic bridging ligands: synthesis, characterization, and intramolecular quenching of MLCT excited states. Inorg Chem 2002; 41: 2471-6.

40.   Kim M-J. Chiral Metallodendrimers and oligomers Containing Ru(II) Polypyridyl Complexes [Ph. D.]. Arlington, TX: University of Texas at Arlington; 2000.

41.   Singhal SS, Singhal J, Yadav S, Dwivedi S, Boor PJ, Awasthi YC, et al. Cancer Res 2007; 67: 4382-9.

42.   Singhal SS, Singhal J, Yadav S, Dwivedi S, Boor PJ, Awasthi YC, et al. Regression of lung and colon cancer xenografts by depleting or inhibiting RLIP76 (ral-binding protein 1). Cancer Res 2007; 67: 4382-9.

43.   Mohler DL, Downs JR, Hurley-Predecki AL, Sallman JR, Gannett PM, Shi X. DNA Cleavage by the Photolysis of Cyclopentadienyl Metal Complexes: Mechanistic Studies and Sequence Selectivity of Strand Scission by $CpW(CO)_3CH_3$. J Org Chem 2005; 70: 9093-102.

44.   Pratviel G, Bernadou J, Meunier B. DNA and RNA cleavage by metal complexes. Adv Inorg Chem 1998; 45: 251-312.

45.   Janaratne TK. Investigation of Ruthenium (II) Polypyridyl Dimers as Potential Chemotherepeutic Agents [Ph. D. thesis]. Arlington, TX: University of Texas at Arlington; 2006.

46.   Rajput C, Rutkaite R, Swanson L, Haq I, Thomas JA. Dinuclear monointercalating RuII complexes that display high affinity binding to duplex and quadruplex DNA. Chem Eur J 2006; 12: 4611-9.

47.   de Tacconi NR, Lezna RO, Chitakunye R, MacDonnell FM. Electroreduction of the Ruthenium Complex [$(bpy)_2Ru(tatpp)$)]Cl_2 in Water: Insights on the Mechanism of Multielectron Reduction and Protonation of the Tatpp Acceptor Ligand as a Function of pH. Inorg Chem 2008; 47: 8847-58.

23

48.   de Tacconi NR, Lezna RO, Konduri R, Ongeri F, Rajeshwar K, MacDonnell FM.

Influence of pH on the photochemical and electrochemical reduction of the dinuclear ruthenium

complex, [(phen)$_2$Ru(tatpp)Ru(phen)$_2$]Cl$_4$, in water: Proton-coupled sequential and concerted

multi-electron reduction. Chem Eur J 2005; 11: 4327-39.

Table 1   **IC$_{50}$ of Ru (II) polypyridyl complexes (H358 and H226)**

Complex	Abbr.	IC$_{50}$ (µM) H358	IC$_{50}$ (µM) H226
rac-[Ru(phen)$_3$]$^{2+}$	**1**$^{2+}$	86.7 ± 4.1	92.8 ± 5.7
Δ-[Ru(phen)$_3$]$^{2+}$	Δ-**1**$^{2+}$	64.8 ± 4.2	93.6 ± 6.3
Λ-[Ru(phen)$_3$]$^{2+}$	Λ-**1**$^{2+}$	61.4 ± 4.7	116 ± 6.9
rac-[Ru(bpy)$_3$]$^{2+}$		209 ± 16	198 ± 15
rac-[(phen)$_2$Ru(tatpp)]$^{2+}$	**3**$^{2+}$	13.2 ± 1.8	12.5 ± 1.9
Δ-[(phen)$_2$Ru(tatpp)]$^{2+}$	Δ-**3**$^{2+}$	8.8 ± 1.0	6.7 ± 1.0
Λ-[(phen)$_2$Ru(tatpp)]$^{2+}$	Λ-**3**$^{2+}$	13.8 ± 1.5	13.0 ± 2.0
mix-[(phen)$_2$Ru(tatpp)Ru(phen)$_2$]$^{4+}$	**4**$^{4+}$	15.2 ± 1.8	16.2 ± 1.9
ΔΔ-[(phen)$_2$Ru(tatpp)Ru(phen)$_2$]$^{4+}$	ΔΔ-**4**$^{4+}$	9.5 ± 1.2	9.3 ± 0.9
ΛΛ-[(phen)$_2$Ru(tatpp)Ru(phen)$_2$]$^{4+}$	ΛΛ-**4**$^{4+}$	16.7 ± 1.0	17.3 ± 1.5
ΔΛ-[(phen)$_2$Ru(tatpp)Ru(phen)$_2$]$^{4+}$	ΔΛ-**4**$^{4+}$	15.3 ± 1.5	18.6 ± 1.5
mix-[(phen)$_2$Ru(tpphz)Ru(phen)$_2$]$^{4+}$	**2**$^{4+}$	41.8 ± 2.7	51.1 ± 3.4
rac-[(phen)$_2$Ru(tpphz)]$^{2+}$		44.0 ± 3.0	49.2 ± 3.1

25

Table 2   DTP COMPARE Analysis[1]: Mechanism of Action of RPC Δ-3^{2+} (NSC 747949)

Class	Drug	Correlation
Antimitotic Agent	Paclitaxel	0.91
	Vincristine	0.55
	Echinomycin	0.49
RNA/DNA Antimetabolite	Pyrazofurin	0.67
	5-FUDR	0.53
	5-fluorouracil	0.53
	Ftoafur	0.52
	Thioguanine	0.41
Alkylating Agent	Cyclodisone	0.62
	Piperazine alkylator	0.57
	Mitomycin C	0.52
	Porfiromycin	0.51
	CCNU	0.50
	Cisplatin	0.47
	Chlorambucil	0.43
	Thio-tepa	0.43
	Tetraplatin	0.42
	Chlorozotocin	0.40
Topo II	"N, N-dibenzyldaunomycin"	0.52

[1]The DTP Compare Analysis uses cytotoxicity data for the test-drug across the NCI-60 spectrum of cell lines to determine is a correlation coefficient of measurement of the similarity in cytotoxic mechanism between the test subject drug, and known cytotoxic drugs with known mechanisms of action. The correlation coefficient ranging from 0 to 1 reflects the degree of similarity. Thus the above findings indicate maximum similarity of mechanism to paclitaxel and significant similarity to several drugs across the antimetabolite and alkylating agent class.

Table 3   MTDs of Ru (II) polypyridyl complexes in C57 BL/6 mice

Complex (chloride salt)	**Abbr.**	**Maximum Tolerable Dose** MTD μmol complex /kg mouse (mg complex /kg mouse)
rac-[Ru(phen)$_3$]$^{2+}$	**1**$^{2+}$	9.1 (6.6)
rac-[(phen)$_2$Ru(tatpp)]$^{2+}$	**3**$^{2+}$	65 (67)
mix-[(phen)$_2$Ru(tatpp)Ru(phen)$_2$]$^{4+}$	**4**$^{4+}$	43 (66)
$\Delta\Delta$-[(phen)$_2$Ru(tatpp)Ru(phen)$_2$]$^{4+}$	$\Delta\Delta$-**4**$^{4+}$	64 (100)
$\Lambda\Lambda$-[(phen)$_2$Ru(tatpp)Ru(phen)$_2$]$^{4+}$	$\Lambda\Lambda$-**4**$^{4+}$	43 (66)
$\Delta\Lambda$-[(phen)$_2$Ru(tatpp)Ru(phen)$_2$]$^{4+}$	$\Delta\Lambda$-**4**$^{4+}$	43 (66)
mix-[(phen)$_2$Ru(tpphz)Ru(phen)$_2$]$^{4+}$	**2**$^{4+}$	2.5 (3.3)

27

FIGURE LEGENDS

Fig. 1   Ruthenium-polypyridyl complexes (RPCs) and associated ligand

structures.   The chemical structure of the important ligands and RPCs, $\mathbf{1}^{2+}$, $\mathbf{2}^{4+}$, $\mathbf{3}^{2+}$, and $\mathbf{4}^{4+}$,

in this study are shown. Chloride counterions are not shown. All of the complexes are chiral

due to the three-fold helical chirality at the ruthenium centers, shown schematically for RPC $\mathbf{1}^{2+}$.

These RPCs are isolated as a racemic mixture for the monomers ($\mathbf{1}^{2+}$ and $\mathbf{3}^{2+}$) or as

diastereotopic mixture of stereoisomers ($\Delta\Delta$, $\Lambda\Lambda$ and $\Delta\Lambda$) for the dinuclear complex ($\mathbf{2}^{4+}$ and $\mathbf{4}^{4+}$).

In certain cases, the RPCs were prepared in diastereomerically and enantiomerically pure

forms, i.e., Δ-$\mathbf{1}^{2+}$ and Λ-$\mathbf{1}^{2+}$, Δ-$\mathbf{3}^{2+}$ and Λ-$\mathbf{3}^{2+}$, $\Delta\Delta$-$\mathbf{4}^{4+}$, $\Lambda\Lambda$-$\mathbf{4}^{4+}$ and $\Delta\Lambda$-$\mathbf{4}^{4+}$, where the descriptor Δ

or Λ is used to indicate right or left-handed chirality, respectively, at the ruthenium centers.

Fig. 2 Hypoxia-Selective, anti-proliferative and pro-apoptotic effect of ruthenium

compounds in human NSCLC.   H358m cell count after incubation with Δ-$\mathbf{3}^{2+}$, cisplatin, and

$[Ru(phen)_2(dppz)]^{2+}$ (DPPZ) for 24 h in hypoxic (1 % O_2) and non-hypoxic incubators (filled and

open symbols, respectively). Cells were checked every 4 h to ensure viability. Complex

concentrations were made prior to inoculation to ensure consistent time. Cell viability was

counted using a hemocytometer w/ Trypan blue staining. 5 dishes were used per set of different

concentrations from 0.01 - 100 µM in the cell medium and were put in respectively in 25 min

increments to allow cell counting with respect to 24 h mark for each cell set. (**panel A**).

Inhibitory effect of ruthenium compounds Δ-$\mathbf{3}^{2+}$ and $\Delta\Delta$-$\mathbf{4}^{4+}$ on cell cycle distribution was

determined by FACS analysis (**panel B**). For in situ caspase-cleavage assay, normal (HUVEC)

and lung cancer (H358) cells (0.1×10^6) were grown on glass cover-slips and treated with either

10 µM of Δ-$\mathbf{3}^{2+}$ and $\Delta\Delta$-$\mathbf{4}^{4+}$ for 12 h and caspase-cleavage was measured using caspase FITC-

VAD-FMK kit. Activated caspase-positive cells appeared fluorescing green and pink when co-

28

stained with DAPI. For detection of late event of apoptosis, TUNEL apoptotic assay was performed. Green fluorescence represents apoptotic cells (**panel C**). The effect of Δ-**3**$^{2+}$ and $\Delta\Delta$-**4**$^{4+}$ on PARP-cleavage in H358 cells and on apoptotic, proliferative, and tumor suppressor proteins was assayed. H358 cells, control, and treated (10 µM either Δ-**3**$^{2+}$ and $\Delta\Delta$-**4**$^{4+}$ for 24 h), were lysed and analyzed by Western blot by using specific antibodies for each protein. Membranes were stripped and re-probed for GAPDH as a loading control (**panel D**).

Fig 3. GSH-stimulated hypoxic DNA Cleavage by RPCs.   DNA cleavage assay showing conversion of supercoiled pUC18 plasmid DNA to circular DNA upon treatment with GSH and Δ-**3**$^{2+}$ or $\Delta\Delta$-**4**$^{4+}$ under aerobic and anaerobic (3 ppm O_2) conditions (**panel A**) DNA cleavage of GSH and Δ-**3**$^{2+}$ under anaerobic conditions in the presence of DMSO (oxygen radical scavinger) and TEMPO (carbon or metal-based radical scavinger) (**panel B**). In each figure, the upper band is the circular (cleaved) plasmid and the lower band is the (uncleaved) supercoiled plasmid.

Fig. 4 Effect of ruthenium compounds on H358 human lung cancer nude mice xenograft model   Hsd: Athymic nude nu/nu mice were obtained from Harlan, Indianapolis, IN. All animal experiments were carried out in accordance with a protocol approved by the Institutional Animal Care and Use Committee (IACUC). Nine 10-week-old nude mice were divided into three groups of 3 animals (treated with PBS (pink), ruthenium compound Δ-**3**Cl$_2$ (green) and $\Delta\Delta$-**4**Cl$_4$ (blue) (70 mg / kg b.w.). All 9 animals were injected with 1 x 10^6 human lung cancer cells (H358) suspensions in 100 µl of PBS, subcutaneously into one flank of each nu/nu nude mouse. At the same time, animals were randomized treatment groups as indicated in the figure. Treatment was administered when the tumor surface area exceeded ~ 42 mm^2 (day 24).

29

Treatment consisted of Δ-**3**$^{2+}$ (2 mg) and $\Delta\Delta$-**4**$^{4+}$ (2 mg) in 200 µl PBS. Control groups were treated with 200 µl PBS. Animals were examined daily for signs of tumor growth. Tumors were measured in two dimensions using calipers. Photographs of animals were taken at day 1, day 10, day 20, day 30, and day 60 after treatment, are shown for all groups.
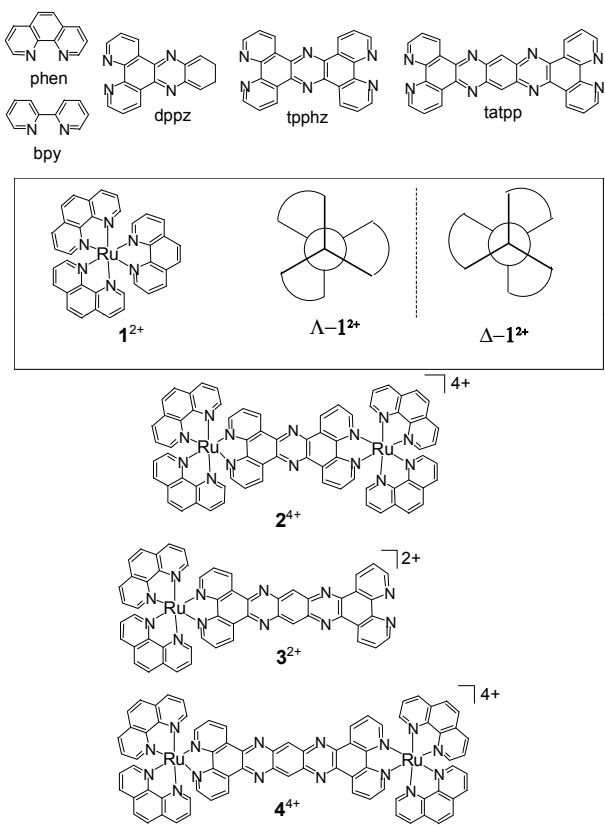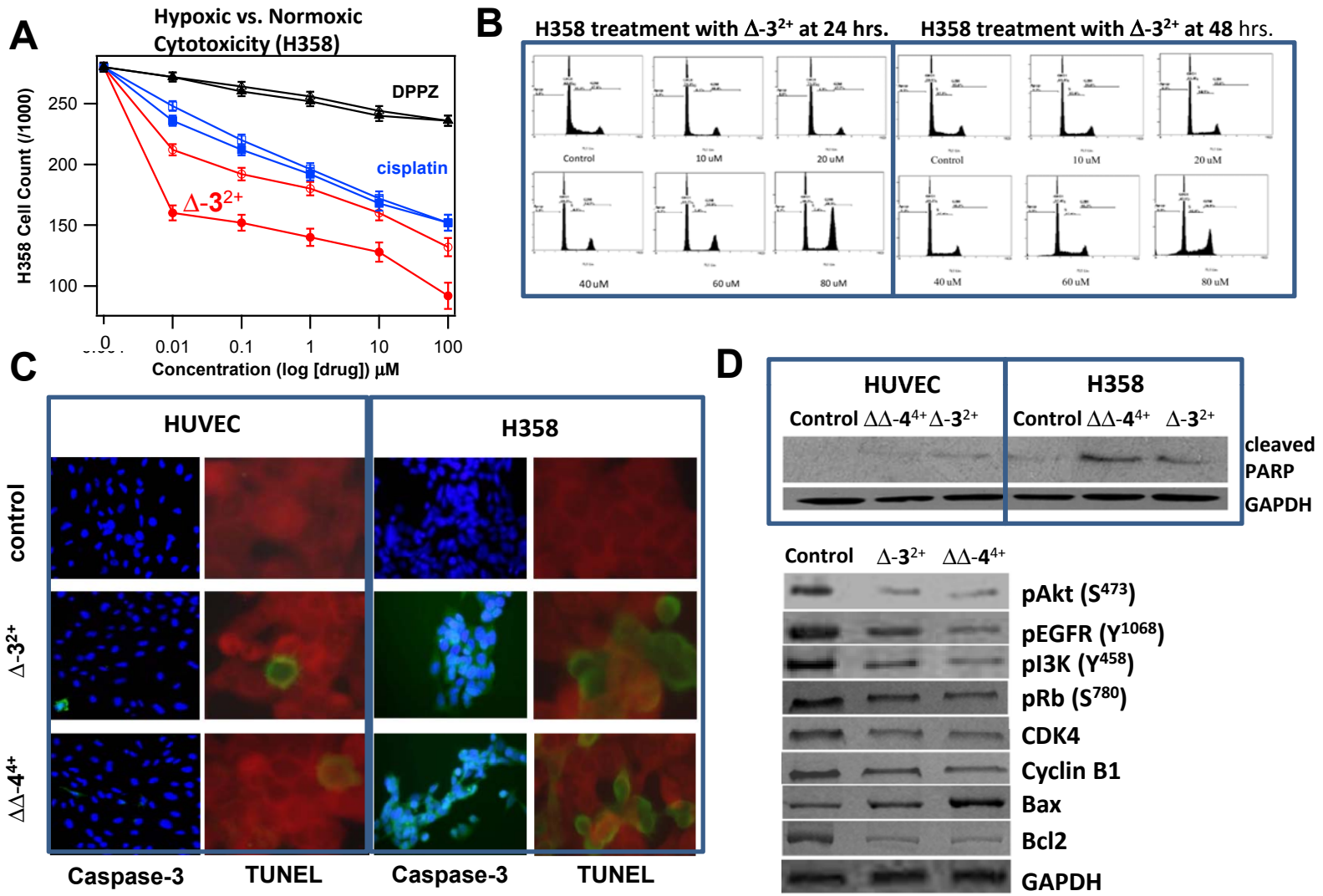
Fig 1

Fig 2

A Hypoxic vs. Normoxic Cytotoxicity (H358)

DPPZ
cisplatin
Δ-3^{2+}

H358 Cell Count (/1000)
Concentration (log [drug]) μM

B H358 treatment with Δ-3^{2+} at 24 hrs.

Control   10 uM   20 uM
40 uM   60 uM   80 uM

H358 treatment with Δ-3^{2+} at 48 hrs.

Control   10 uM   20 uM
40 uM   60 uM   80 uM

C

HUVEC	H358

control
Δ-3^{2+}
$\Delta\nabla$-4^{4+}

Caspase-3   TUNEL   Caspase-3   TUNEL

D

HUVEC		H358	
Control $\Delta\Delta$-4^{4+} Δ-3^{2+}		Control $\Delta\Delta$-4^{4+} Δ-3^{2+}	

cleaved PARP
GAPDH

Control Δ-3^{2+} $\Delta\Delta$-4^{4+}

pAkt (S^{473})
pEGFR (Y^{1068})
pI3K (Y^{458})
pRb (S^{780})
CDK4
Cyclin B1
Bax
Bcl2
GAPDH

Fig 3

A

circular
linearized

supercoiled

pUC18 DNA

	1	2	3	4	5	6	7	8
ΔΔ-4^{4+}			+	+	+			
Δ-3^{2+}						+	+	+
GSH		+		+	+		+	+
O$_2$	+	+	+	+		+	+	

B

circular

supercoiled

pUC18 DNA

	1	2	3	4	5	6
Δ-3^{2+}		+		+	+	+
GSH			+	+	+	+
DMSO						+
TEMPO					+	

Fig 4

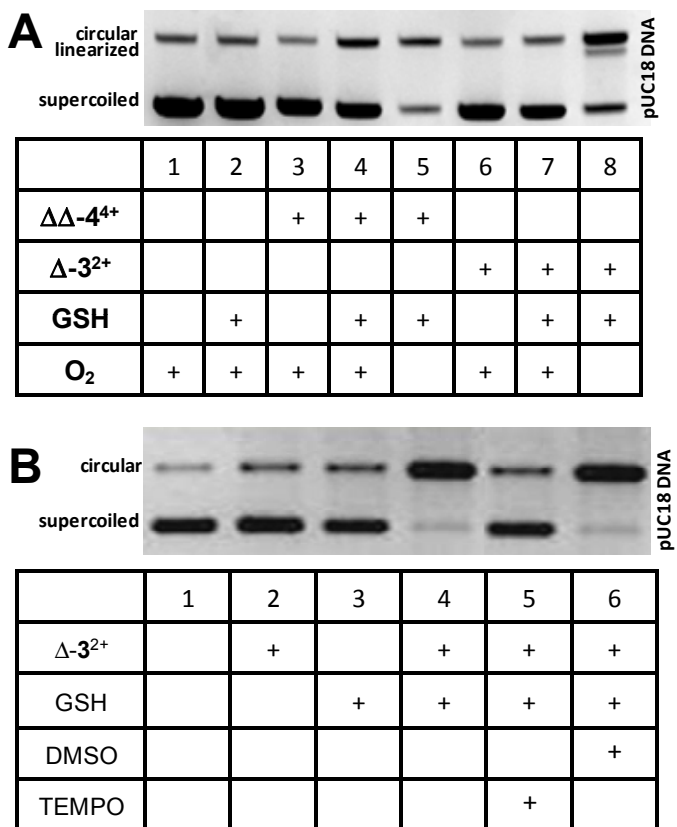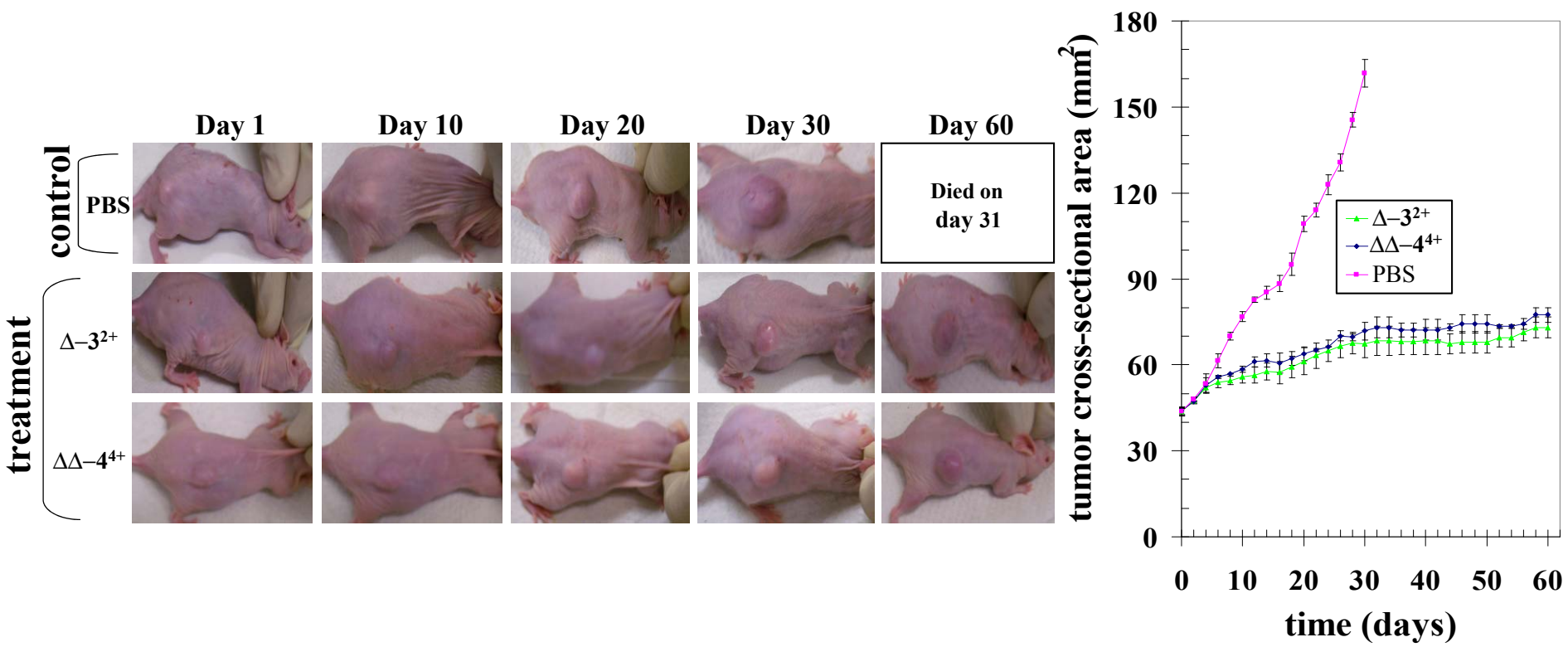AAC-R American Association
for Cancer Research

Molecular Cancer Therapeutics

Regression of Lung Cancer by Hypoxia Sensitizing Ruthenium Polypyridyl Complexes

Abhishek Yadav, Thamara Janaratne, Arthi Krishnan, et al.

Updated version	Access the most recent version of this article at: doi:10.1158/1535-7163.MCT-12-1130
Author Manuscript	Author manuscripts have been peer reviewed and accepted for publication but have not yet been edited.

E-mail alerts	Sign up to receive free email-alerts related to this article or journal.
Reprints and Subscriptions	To order reprints of this article or to subscribe to the journal, contact the AACR Publications Department at pubs@aacr.org.
Permissions	To request permission to re-use all or part of this article, use this link http://mct.aacrjournals.org/content/early/2013/02/26/1535-7163.MCT-12-1130. Click on "Request Permissions" which will take you to the Copyright Clearance Center's (CCC) Rightslink site.